

# PROJECT VALVERDE – VALIDATION AND VERIFICATION OF COMPUTATIONAL TOOLS TO DESCRIBE CORIUM SPILL TO IMPROVE DETERMINISTIC ANALYSES OF SEVERE ACCIDENTS

JAN KOMRSKA\*, PAVEL PEKÁREK, TOMÁŠ HOPPE, PAVEL ZÁCHA

*Czech Technical University in Prague, Faculty of Mechanical Engineering, Department of Energy Engineering, Technická 4, 160 00 Prague 6, Czech Republic*

\* corresponding author: [jan.komrska@fs.cvut.cz](mailto:jan.komrska@fs.cvut.cz)

**ABSTRACT.** The VALVERDE project focuses on the investigation of the melt flow characteristics of the core melt simulant material and the subsequent development of suitable procedures and methodologies for the description of the melt flow of the simulant in a defined geometry. The main aim is to develop an experimental setup in which the melt spreading of the corium will be performed using suitable simulants. The current version of the experimental setup and the CFD simulations of the spreading of the reactor core melt simulant will be presented.

**KEYWORDS:** Corium, melt spreading, corium simulant, CFD.

## 1. INTRODUCTION

Using corium simulants in the research of corium spreading behavior is essential because working with real corium is extremely hazardous and complex. Corium is a highly radioactive, molten mixture of nuclear fuel, fission products, reactor core materials, and structural metals formed during a severe nuclear reactor accident, such as a core meltdown. Its temperature can exceed 2000 °C, making it capable of melting through steel and concrete structures [1].

The composition of corium depends on the type of reactor and accident conditions but generally includes uranium dioxide fuel, cladding materials, stainless steel, control rod materials, and various oxides formed during interactions with coolant and structural components. Because it is both thermally aggressive and chemically reactive, corium can interact with reactor pressure vessel walls and containment basemats, potentially leading to melt-through and release of radionuclides into the environment [1].

Studying its behavior is therefore critical for nuclear safety, especially in understanding and improving core catchers (specialized components designed to cool and contain corium if it breaches the reactor pressure vessel), containment strategies, and accident mitigation systems. Research focuses on how corium spreads, cools and solidifies, as well as how it reacts with water and concrete, since these interactions can produce explosive gases like hydrogen and carbon monoxide.

Because of the extreme risks involved, researchers use corium simulants – non-radioactive materials that mimic corium’s flow, spreading, and solidification characteristics under high-temperature conditions. These experiments provide valuable insights that guide the design of safer nuclear reactors and enhance emergency preparedness in the event of severe accidents. Project VALVERDE (VALidation and VERification

of computational tools to describe corium spill to improve DETERministic analyses of severe accidents) is dedicated to investigating corium melt spreading, with emphasis on both flow dynamics and solidification front propagation, followed by the validation and verification of computational models for simulating these processes. To experimentally reproduce the relevant phenomena, a suitable simulant is required. After a comparative evaluation, paraffin wax was identified as the most appropriate choice. Although its thermophysical properties do not fully replicate those of real corium, paraffin provides a low-cost, low-hazard analogue that reliably captures the dominant mechanisms of interest, particularly spreading behavior and solidification kinetics, under well-controlled and observable laboratory conditions.

In this paper, the current version of the experimental setup and the computational fluid dynamics (CFD) simulations of the spreading of the reactor core melt simulant used optimization of the design of the experiment are presented.

## 2. EXPERIMENTAL SETUP

The VALVERDE experimental stand is designed to simulate and analyze the dynamics of molten wax flows under controlled conditions. The system is composed of three principal components: wax heating system, adjustable outflow system, and simulant spreading area, each serving a specific function within the overall experimental framework. The experimental setup is shown in Figure 1.

### 2.1. WAX HEATING SYSTEM

The first component is a thermal control system dedicated to heating and maintaining paraffin wax in a fully molten state. The wax is housed in a thermally insulated container, where it is maintained at

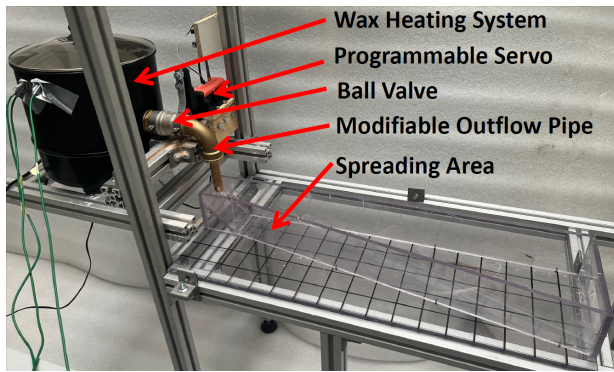


FIGURE 1. VALVERDE experimental stand.

a predetermined temperature to ensure consistency across experimental runs. Temperature regulation and monitoring are achieved through the integration of K-type thermocouples, which are strategically positioned within the heating chamber to provide accurate and real-time thermal data. These thermocouples serve as a crucial source of reference for both experimental observations and model validation.

### 2.2. ADJUSTABLE OUTFLOW SYSTEM

The second component involves a modifiable outlet conduit that facilitates the release of the molten wax into the test domain. This system includes a programmable servo motor coupled to a precision-controlled ball valve, which governs the timing and duration of wax discharge. The outlet pipe can be easily interchanged to accommodate different internal diameters, allowing for systematic investigation of flow behavior as a function of outlet geometry. This modular design supports a variety of experimental configurations and contributes to the reproducibility of the results.

### 2.3. SIMULANT SPREADING AREA

The third component comprises the flow spreading surface, which is demarcated using a  $5 \times 5$  cm square mesh grid. This grid serves as a spatial reference to enhance the clarity and quantitative assessment of the spreading behavior during and after wax release. The grid also helps in tracking the evolution of flow fronts and pattern formation over time. Transparent material was chosen for the wall and spill area to allow better observation of the spill from below and at selected angles.

The spread geometry follows the design of the VULCANO VE-U7 [2] experiment spill area. The main reasons for choosing this geometry were the success of the VE-U7 experiment, against which some computational codes were validated. At the same time, it is an experiment that has been extensively described, and the results from the VALVERDE experiment can be compared with it.

To facilitate high-resolution data acquisition, the experimental setup is further equipped with two high-

speed cameras positioned at different angles to capture rapid transient events and a thermal imaging camera that provides detailed spatial temperature distributions during the flow process. Additional K-type thermocouples are embedded within the spreading area to capture surface temperature variations, which are also used as boundary and validation data for CFD simulations.

## 3. PREPARATORY CFD SIMULATIONS

The CFD model created for use in ANSYS Fluent 2024R1 [3] was developed based on the initial design of the experimental device. The purpose of the simulations was to make initial estimates of the starting temperature of the paraffin and to monitor the process by which the paraffin simulant enters the channel and how it subsequently spreads through the spreading area. CFD simulations were performed for 35 mm diameter outflow pipe to optimize the experiments based on a fixed initial velocity of  $1.5 \text{ m s}^{-1}$  and a varying initial temperature.

### 3.1. CASE GEOMETRY

The geometry of the computational model was created in ANSYS SpaceClaim and is based on the design of the VALVERDE spreading channel. The overall dimensions of the model are  $825 \times 200.16 \times 200$  mm. The inlet (shown in green) was moved 100 mm while maintaining a diameter of 35 mm so that the inlet flow of the simulant would be more developed and stable for the calculation. The inlet pipe is centered on a  $75 \times 75$  mm beveled surface with a  $45^\circ$  bevel from the base plate. The beveled surface serves to direct the flow in the direction of the expanding channel. The height of the walls surrounding the model is 100 mm. The spillway itself is 750 mm long with an inlet width of 75 mm and a width of 200.16 mm at the end of the channel, giving a total area of  $0.103 \text{ m}^2$ . Dimensions of the geometry of the computational area are described in Figure 2. The outlet is located on an imaginary ceiling at the end of the channel and serves as a gas outlet to prevent overpressure in the channel during calculation when it is actually open to atmospheric pressure. Both inlet and outlet areas are shown in Figure 3.

### 3.2. MESH SENSITIVITY ANALYSIS

Mesh sensitivity analysis was performed for several meshes of varying degrees of cell dimensions. This is done to find the optimal mesh size that allows quick computational times but doesn't sacrifice any important solution accuracy of observed physical phenomena. All computational meshes consist of three regions. These are the region of prismatic cells in the boundary layer, the region of finer cells for paraffin flow, and the region of coarse cells for gas flow, which in our case is air at atmospheric pressure. This division allows us to minimize the number of cells in the airflow region and maximize the number of finer cells

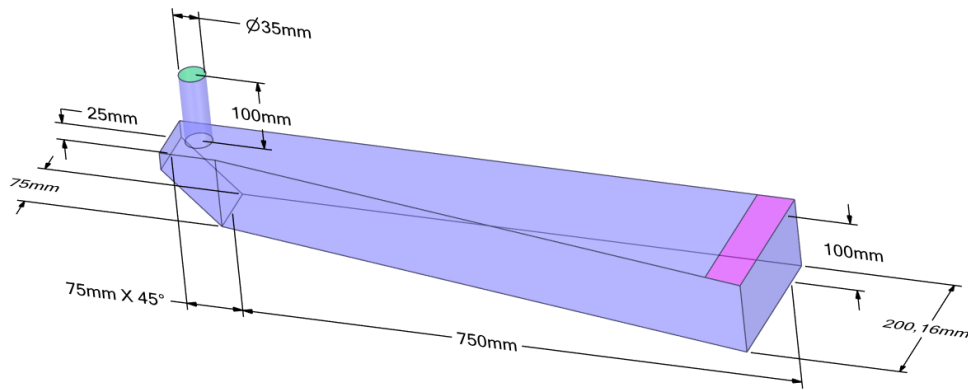


FIGURE 2. Case geometry.

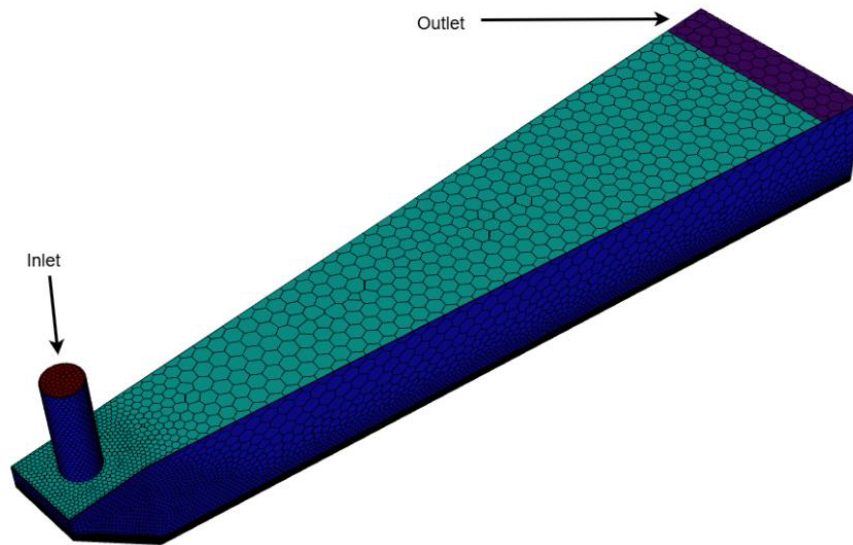


FIGURE 3. Isometric view of computational mesh.

needed for better resolution in the paraffin flow region. The maximum cell size in this coarse airflow region was set at 30 mm. The finer area, where paraffin flow is expected, was created using the BOI (Body of Influence) function, which allows us to set the maximum cell size and cell growth factor for the selected volume. The finer cell region is mainly in the channel inlet area and then above the spill area up to a height of 20 mm. The last area consists of prismatic cells rising from the sloped surface and the spill area. These are uniform cells whose size is determined by the BOI value, height  $P$ , and number of layers. The total height of this region was set to 8 mm. This approach to mesh creation using finer meshing details can be seen on Figure 4.

A total of four meshes with different maximum dimensions in the BOI area were examined, ranging from 6 mm for a coarse mesh to 1.5 mm for a very fine mesh. At the same time, for BOI 4 mm, the influence of the fineness of the height of the prismatic cells was examined for double and half the number of prismatic cells while maintaining the total height of this region at 8 mm. The volume cells were generated

as polyhedral and their number ranged from 100 000 to 2 000 000 for individual meshes.

The quality of all the meshes created was sufficient, with a minimum orthogonal quality value greater than 0.35.

### 3.3. CFD CASE DESCRIPTION AND SETTINGS

The settings for a suitable numerical model are based mainly on the experience gained while working with similar types of simulations [4]. A basic overview of the schemes and numerical models used can be found in the following Table 1.

The viscosity of the paraffin intended for experimental use was examined on a viscometer, and the results roughly correspond to the values given in references [5]. The viscosity values are given at 5 °C, and the lowest temperature at which the viscosity was measured corresponded to 60 °C. At lower temperatures, the paraffin had already solidified. The exact solidification temperature is unknown, but it occurs between 55 °C and 60 °C. In the material properties settings, the temperature-dependent properties were defined using the Piecewise-Linear function, where the pro-

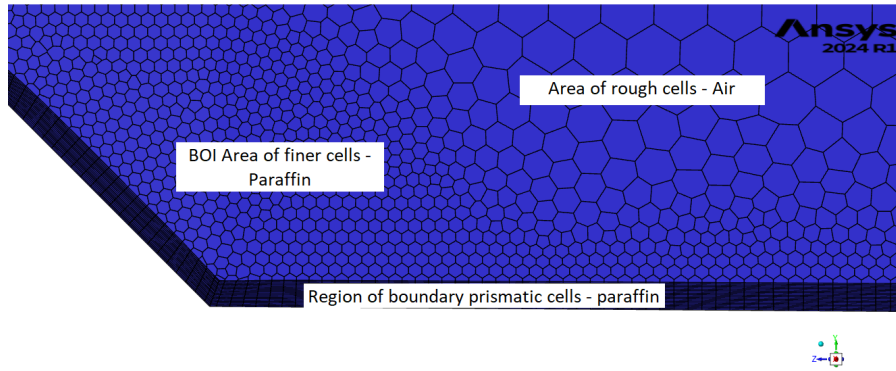


FIGURE 4. Detail of various regions of the mesh.

Parameter	Used scheme/model
Solver type	Pressure Based
Time Dependence	Transient
Solver Precision	3D Double Precision
Multiphase Model	Volume of Fluid
Energy Equation included	Yes
Viscous Model	Standard K-Epsilon
Pressure-Velocity Coupling	Coupled
Gradient	Least Squares Cell
Pressure	PRESTO!
Momentum	First Order Upwind
Volume Fraction	Geo-Reconstruct
Turbulent Kinetic Energy	First Order Upwind
Turbulent Dissipation Rate	First Order Upwind
Energy	First Order Upwind
Transient Formulation	First Order Implicit

TABLE 1. CFD case settings used in the simulation.

Property	Value
Specific heat	$2510 \text{ J (kg K)}^{-1}$
Thermal conductivity	$0.24 \text{ W (m K)}^{-1}$
Dynamic viscosity	Defined in Figure 5
Density	Defined in Figure 6

TABLE 2. Paraffin material properties used in simulation [5].

gram treats the interval between the specified values as linear. To reflect the effect of paraffin solidification during cooling, a viscosity value was artificially created for 55 °C, which corresponds to a viscosity value 100 times greater than that for 60 °C. The specific heat capacity and thermal conductivity of paraffin do not change significantly with temperature, so they were left as constants. Properties of paraffin wax used in the CFD simulation can be found in Table 2 and Figures 5 and 6.

The boundary conditions at the inlet are based on the assumption that the entire volume of paraffin will be heated in a vertical furnace and tube and, once the temperature is reached, discharged into the experimental spreading channel by quickly opening the

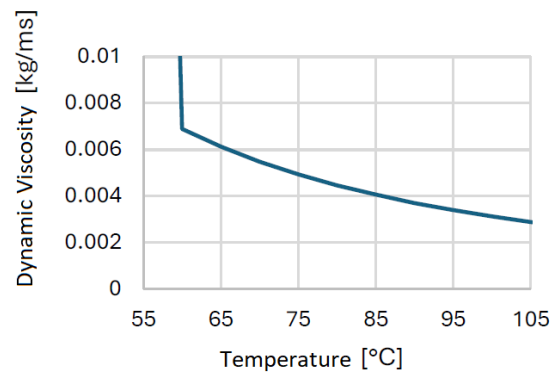


FIGURE 5. Piece-wise linear function describing dynamic viscosity of paraffin wax.

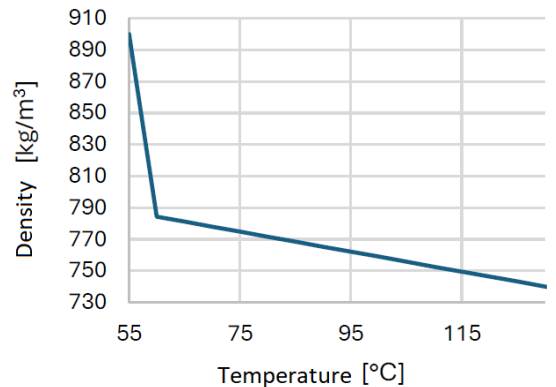


FIGURE 6. Piece-wise linear function describing density of paraffin wax.

inlet plate (i.e. ball valve). The amount of paraffin used in the simulation was calculated from the volume of corium discharged into one channel in the VE-U7 experiment [2]. An average of 13 kg of corium flowed in one channel with an approximate density of  $7140 \text{ kg m}^{-3}$ , which corresponds to approximately  $0.0018 \text{ m}^3$ . For the same volume, the weight of paraffin corresponds to 1.43 kg. For our calculations, a quarter of the amount of paraffin was chosen, which corresponds to 0.357 kg and a volume of  $4.55 \cdot 10^{-4} \text{ m}^3$  at 60 °C. The maximum height of paraffin in a pipe with a diameter of 35 mm is approximately 0.473 m.

Boundary condition	Value
Inlet Boundary Condition	Velocity Inlet
Inlet Velocity Profile	Defined in Figure 7
Inlet Temperature	Case-Dependent
Inlet Velocity	$1.5 \text{ m s}^{-1}$
Outlet Boundary Condition	Pressure Outlet
Backflow Temperature	293.15 K
Wall Temperature	293.15 K
Wall Width	10 mm

TABLE 3. Basic CFD case settings.

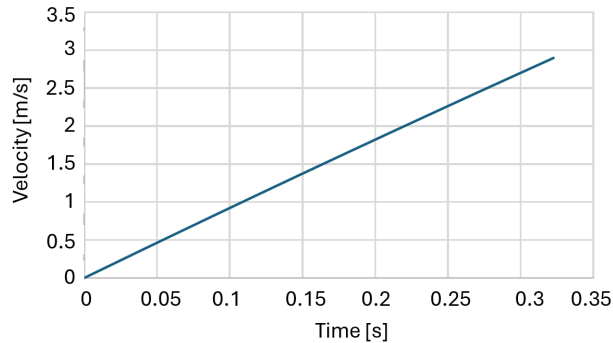


FIGURE 7. Piece-wise linear function describing inlet boundary condition velocity increase to make a more realistic approach of ball valve opening.

A summary of the basic boundary conditions is given in the following Table 3.

### 3.4. MESH SENSITIVITY ANALYSIS RESULTS

In the first part of the sensitivity analysis, four meshes with a constant prismatic cell height of P 0.4 mm and varying maximum cell sizes in BOI of 6 mm and 1.5 mm were compared. The basic parameters monitored in the sensitivity analysis were the time it took for the paraffin to reach the end of the channel, the area covered by the paraffin at the time of reaching the end and the average height of the paraffin in the spill channel at the time of touching the end of the experimental channel.

The time at which the paraffin component touches the wall at the end of the channel varies in units of thousands of seconds. A greater difference in the results can be observed in the flooded spreading area for a uniform time of 0.7 s. The trend of the flooded area increases with time with greater mesh fineness. From the selected base value for the BOI 4 mm, P 0.4 mm mesh, the area flooded with paraffin for the coarse mesh differs by more than 10 % and by 6.5 % for the very fine mesh. Results of the mesh analysis for fixed P dimension can be seen on Figure 8 and on Figure 9 we can observe the paraffin spreading for BOI 4 mm, P 0.4 mm case. The average paraffin level at the end of the channel differs more significantly within 150 mm of the inlet to the spread area. The difference in heights is due to the different adhesion of paraffin to the walls and the speed of flow from the sloped surface, which

creates a secondary wave entering the spread area. Further in the channel, where the flow is already fully developed, the paraffin level profile is practically the same for all computational meshes examined.

In terms of computational cost, a significant difference was observed between mesh resolutions: simulations with a very fine mesh (BOI 1.5 mm, P 0.4 mm) required over one hour to compute just 0.01 s of physical time, whereas coarser meshes completed the same interval within minutes. For subsequent analyses, the basic mesh (BOI 4 mm, P 0.4 mm) was selected as the optimal compromise, providing a satisfactory balance between solution accuracy and computational efficiency.

### 3.5. INITIAL TEMPERATURE PARAMETRIC STUDY

A parametric study was performed for the optimal mesh selected, focusing on the effect of different input paraffin temperatures on the computational model. The simulation was performed for four different temperatures: 60 °C, 70 °C, 80 °C, and 90 °C. When comparing the spill area flooded, a difference can be observed mainly between the inlet temperature of 60 °C, where slightly over 80 % is flooded in 0.7 s, and the other temperatures, where almost the entire channel area is flooded in 0.7 s. The spread profile for temperatures from 70 °C to 90 °C is very similar and differs slightly in the speed at which the end of the channel is reached, with the most superheated simulant also being the fastest.

The significant difference between the flooded area is represented by viscosity, which changes more significantly when cooled below 60 °C and only slightly when heated above 60 °C. The average height over time is comparable for higher simulant temperatures and differs from 60 °C similarly to the simulation using the solidification model, where we have a higher front profile and a more pronounced and sharper secondary wave caused by runoff from the sloping surface and walls.

At higher temperatures, paraffin does not adhere to the walls and the sloping surface but flows into the spreading channel. In contrast, at a simulant temperature of 60 °C, a small portion of the spilled paraffin settled and solidified in the experimental apparatus, mainly on the sloping surface. The biggest difference at higher temperatures is the subsequent collapse of the rear wall of the channel. These differences are best observed on Figure 10 and 11, where we can see the comparison of paraffin spreading at various initial temperatures. At the final time step, which was determined to be 0.7 s (reference time step when paraffin reaches the end of spreading area at 60 °C) the paraffin washes down the wall to a height of 35 mm at 70 °C, 44 mm at 80 °C and 46 mm at 90 °C.

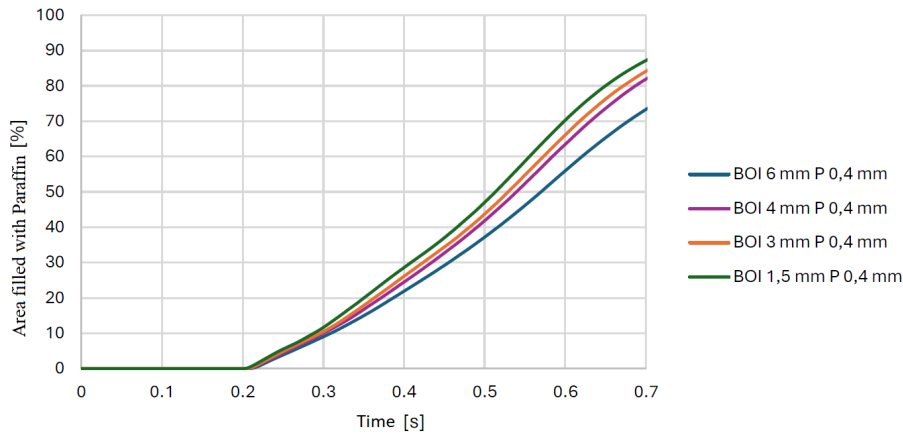


FIGURE 8. Results of mesh sensitivity analysis for fixed  $P = 0.4$  mm dimension.

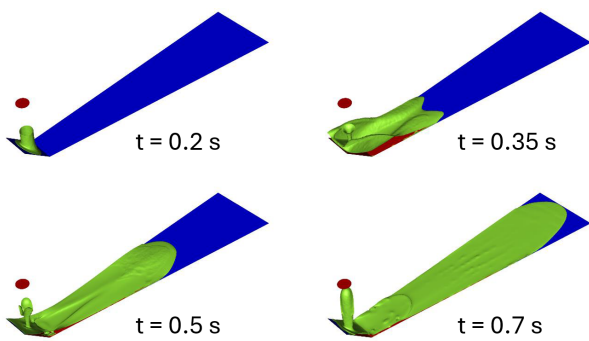


FIGURE 9. Paraffin spreading simulation at various time steps for BOI 4 mm,  $P = 0.4$  mm mesh case.

#### 4. PRE-TEST EXPERIMENTS

Through the application of CFD simulations, the initial boundary and operational conditions of the experimental setup were systematically optimized to achieve more uniform, controlled, and reproducible spreading behavior of the paraffin wax simulant. The simulations allowed for a detailed parametric analysis, focusing in particular on the influence of mass, initial temperature, and valve actuation timing on the flow dynamics and subsequent solidification processes.

The numerical results indicated that the most favorable conditions were obtained to achieve a well-defined spreading front, followed by a timely and observable solidification, when the mass released of the simulant was approximately 100 g and the initial temperature was maintained close to 60 °C. This temperature, which is only slightly above the known solidification point of paraffin wax, allows a short window of flow before the onset of solidification, facilitating a clearer observation of the thermally driven spreading dynamics and phase change behavior.

During the pre-test experimental validation phase, these optimal conditions were closely replicated. The paraffin wax was preheated and released at a temperature of approximately 58 °C, ensuring that it remained in the molten state just long enough to spread before it started to solidify. The programmable valve con-

trol system was actuated with high temporal precision, maintaining an opening duration of exactly 0.5 s. This allowed for the controlled release of 98 g of molten wax, a value closely aligned with the simulation-based recommendation.

The resulting solidified configuration of the paraffin wax simulant, following its discharge onto the spreading surface, is illustrated in Figure 12. The final state of the solidified mass confirms the predictive precision of the CFD simulations and validates the effectiveness of the optimized initial conditions in achieving the desired experimental outcomes.

#### 5. DISCUSSION

The experimental setup, consisting of a wax heating system, modifiable outflow geometry, and a grid-marked spreading area, effectively simulates conditions analogous to corium spreading experiments. The choice of paraffin wax, despite its limited thermal comparability with that of actual corium, is justified by its similar phase transition characteristics and manageable physical behavior. The experimental geometry was inspired by the VULCANO VE-U7 benchmark experiment, ensuring compatibility with previously validated computational codes and providing a valuable baseline for comparative analysis.

The iterative design process of the setup, supported by CFD simulations, highlights the synergy between computational and experimental methods. In particular, the valve-controlled release system allows for precise manipulation of simulant flow parameters, including temperature and mass discharge, thereby increasing reproducibility and control in experimental trials.

The extensive use of CFD modeling in ANSYS Fluent [3], particularly using the volume-of-fluid (VOF) approach, proved crucial in optimizing experimental parameters. A detailed mesh sensitivity analysis confirmed that the simulation results, particularly the paraffin spreading extent and solidification profile, were significantly influenced by grid resolution, particularly in the near-wall and free-surface regions.

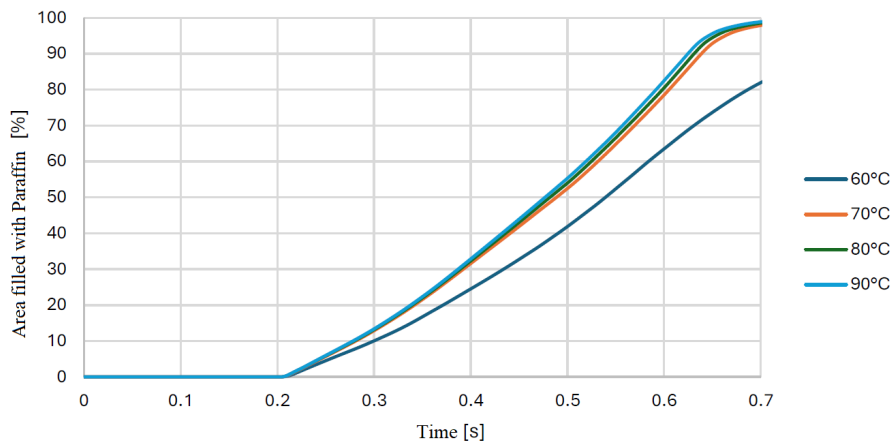


FIGURE 10. Results of paraffin simulant spreading at various initial temperatures.

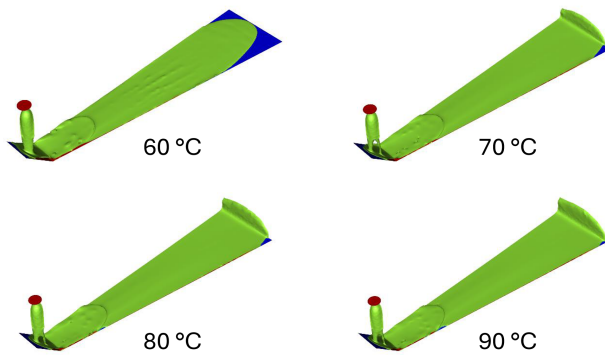


FIGURE 11. Comparison of simulant spreading at various initial temperatures at 0.7 s of simulant spreading.



FIGURE 12. Final state of simulant at the end of pre-test experiment.

However, an optimal mesh (BOI 4 mm, P 0.4 mm) was identified, balancing accuracy and computational efficiency.

Parametric studies on initial temperature revealed non-linear behavior in paraffin viscosity near its solidification point (between 55 °C and 60 °C). As the temperature increased from 60 °C to 90 °C, the simulations showed accelerated spreading, decreased wall adhesion, and increased channel coverage, highlighting the sensitive coupling between thermal and hydrodynamic properties. Interestingly, the greatest variation in the spread dynamics occurred below 60 °C, due to the rapid increase in viscosity that led to premature solidification.

The simulated conditions were validated experimentally by conducting pre-tests under controlled parameters. Releasing 98 g of paraffin at approximately 58 °C allowed direct observation of a well-defined solidification front and provided compelling evidence that the CFD models were predictive and reliable. This level of precision underscores the strength of the modeling approach and supports its application in reactor safety design contexts.

## 6. CONCLUSION

The VALVERDE project represents a methodical and innovative approach to addressing a critical safety challenge in nuclear engineering: understanding the spreading behavior of corium during severe nuclear reactor accidents. Given the inherent hazards associated with real corium, the project utilizes paraffin wax as a low-risk simulant to replicate core melt flow and solidification phenomena in a controlled laboratory environment.

CFD simulations refined the experimental setup by identifying the need to reduce the initial flow rates to control the rapid paraffin outflow and ensure stable spread. To replicate realistic solidification behavior, paraffin wax was released slightly above its solidification point, promoting a distinct solidification front and allowing a clearer analysis of the spreading dynamics.

As a result of the simulation insights, the release system was iteratively redesigned and finalized. The modified system was subsequently tested and yielded promising experimental results, demonstrating reliable flow control and reproducibility.

The CFD models developed within this project will also serve as a foundational tool for validated and verified simulations of corium spreading, specifically supporting the core catcher design for the GFR ALLEGRO reactor.

Despite its strengths, the paraffin-based analogy remains limited in its ability to replicate the extreme thermophysical and radiological conditions of real corium. Moreover, the simplifications involved in the CFD model, such as constant thermal conductivity and artificially scaled viscosity functions, may limit the model's fidelity under more realistic scenarios. Future research could aim to incorporate more advanced material models, multiphase interactions with reactive substrates, and scaling to account for higher temperature regimes.

## ACKNOWLEDGEMENTS

This work was supported by the Czech Technical University SGS Grant – Grant No. SGS24/086/OHK2/2T/12.

## REFERENCES

- [1] B. R. Sehgal. *Nuclear Safety in Light Water Reactors*. Academic Press, 2012.  
<https://doi.org/10.1016/C2010-0-67817-5>
- [2] C. Journeau. The VULCANO VE-U7 Corium spreading benchmark. *Progress in Nuclear Energy* **48**(3):215–234, 2006.  
<https://doi.org/10.1016/j.pnucene.2005.09.009>
- [3] ANSYS. Fluent user's guide, 2024. [2025-09-29].  
[https://ansyshelp.ansys.com/public/account/secured?returnurl=/Views/Secured/corp/v242/en/flu\\_ug/flu\\_ug.html](https://ansyshelp.ansys.com/public/account/secured?returnurl=/Views/Secured/corp/v242/en/flu_ug/flu_ug.html)
- [4] J. Komrska, P. Zácha, P. Vácha. Mesh sensitivity analysis of the CFD model of the core catcher of the ALLEGRO reactor. In *20th International Topical Meeting on Nuclear Reactor Thermal Hydraulics (NURETH-20)*, pp. 3956–3969. 2023.  
<https://doi.org/10.13182/NURETH20-40672>
- [5] A. Paar. Paraffin wax – material properties, 2025. [2025-09-29]. <https://wiki.anton-paar.com/at-de/paraffinwachs/>